IEEE Photonics Journal
An IEEE Photonics Society Publication

Open Access

Ultrafast Wavenumber Linear-Step-Swept Source Based on Synchronous Lightwave Synthesized Frequency Sweeper

Volume 11, Number 1, February 2019

Quan Yuan
Zhaoying Wang
Lipei Song
Chunfeng Ge
Zhaoyu Lu
Tianxin Yang

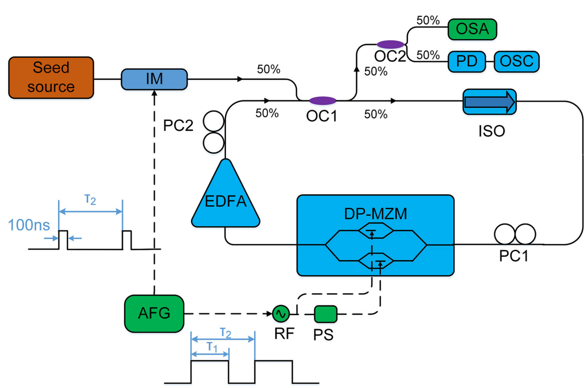

DOI: 10.1109/JPHOT.2019.2894529

IEEE photonics SOCIETY

IEEE

Ultrafast Wavenumber Linear-Step-Swept Source Based on Synchronous Lightwave Synthesized Frequency Sweeper

Quan Yuan ,[1] Zhaoying Wang ,[1] Lipei Song,[2] Chunfeng Ge ,[1] Zhaoyu Lu ,[1] and Tianxin Yang [1]

[1]Key Laboratory of the Ministry of Education on Optoelectronic Information Technology, School of Precision Instrument and Optoelectronics Engineering, Tianjin University, Tianjin 300072, China
[2]Institute of Modern Optics, Nankai University, Tianjin 300350, China

DOI:10.1109/JPHOT.2019.2894529

Manuscript received September 20, 2018; revised January 8, 2019; accepted January 17, 2019. Date of publication January 21, 2019; date of current version February 7, 2019. This work was supported in part by the Natural National Science Foundation of China under Grants 61275084, 61377078, and 61605092 and in part by the Natural Science Foundation of Tianjin City under Grant 18JCYBJC16800.
Corresponding author: Zhaoying Wang (e-mail: wangzy@tju.edu.cn).

Abstract: An ultrafast wavenumber linear-step-swept source based on a synchronous lightwave synthesized frequency sweeper (SLSFS) is demonstrated. A multi-wavelength source is used as a seed source. In SLSFS, the swept range of different wavelength components is precisely controlled by a stable programmable radio frequency signal applied on a dual-parallel Mach–Zehnder modulator instead of a conventional wavelength filter. The identical frequency shifting step of all the wavelength components promises high linear sweeping in the frequency domain. The key significance of this technique is that the swept rate and the swept range increases as the number of the seed wavelengths increases. Experimentally, a 120 kHz swept rate over the 4.75 nm range with a 8.6 GHz swept step is achieved when using two coupled DFB-LDs as the seed source. The K-linearity of Pearson's correlation coefficients is 0.99999. We also acquired the swept rates of 400 kHz, 800 kHz, and 1.23 MHz over the 7.86 nm range with a 8.6 GHz swept step using an F-P LD as a seed source.

Index Terms: Tunable laser, fiber laser, modulator.

1. Introduction

Wavelength-swept source has been widely used in dynamic fiber Bragg grating sensing [1], wavelength-division multiplexing (WDM) networks [2], swept source optical coherence tomography (SS-OCT) [3], frequency-modulated continuous-wave (FMCW) reflectometry [4], dispersion measurement [5], and remote sensing of the atmosphere [6], *etc*. In these systems, a rapid and linear k-space swept source is crucial for increasing the spectrum sampling efficiency and decreasing the complexity of data processing.

Most of the traditional swept lasers use mechanically tuned wavelength filters such as Fabry-Perot tunable filter [7], tunable ratio optical coupler [8], polygon mirror-scanning filter [9], and tunable micro-opto-electro-mechanical system [10] to tune the output wavelength. To increase the repetition rate of a swept laser, the tunable filters need be driven by a sinusoidal signal rather than a linear signal. A general challenge is that both the swept rate and the linearity of swept lasers are limited by the mechanical tuning filters. Even the swept laser exhibits linearity in wavelength over time, its output is still nonlinear in frequency domain (k-space) due to the relationship of $k = 2\pi/\lambda$. For obtaining the linearly sampled data in k-space, such as in SS-OCT system, the output of the swept laser has to be recalibrated in k-space, which introduces a bulk volume and a high cost to the system. Meanwhile, as the increasing of swept rate, the recalibration becomes more complex and time-consuming. In recent research, several wavenumber swept systems have been proposed to increase the linearity of the swept source in k-space including Fourier domain mode locked laser [11], MEMS-tunable VCSEL lasers [12], active mode locking fiber laser [13], verinier-tuned distributed Bragg reflector(VT-DBR)[14] and linear-in-wavenumber swept laser based on an acousto-optic deflector [15]. In [14], the swept rate of VT-DBR is 200 kHz with high linearity in k-space. In [15], the swept linearity is 0.99990 in k-space. However, the systems mentioned above are all a single wavelength swept source. In recent years, a theory using multiple seed source for a swept source is proposed [16]. It attracts many interests for imaging implements such as FMCW and SS-OCT to improve the axial resolution [17], [18]. In addition, multiple wavelength swept source will be very suitable for synchronously interrogating the multiplexed FBG sensors [19].

The lightwave synthesized frequency sweeper (LSFS) is another effective scheme that realizes linear swept output in k-space [20]–[22]. The LSFS consists two main parts: (i) a frequency-stabilized optical seed source; (ii) an optical loop including a frequency shifter and an optical amplifier. The frequency of the incident optical seed signal is shifted by a constant value, which called swept step in the LSFS. Since the swept step is constant, the high linearity of the output signal in frequency domain is guaranteed. Generally, the signal to noise ratio (SNR) of the output decreases with the circulation number increasing due to the noise accumulation induced by the optical amplifier. In [22], a wavelength band-pass filter is used to control the circulation number and an extra optical switch is used to suppress the noise in each circulation. The swept range is 6.1 nm/7.2 nm with a 20 GHz/30 GHz swept step. In LSFS, the frequency modulating is outside of the cavity of the seed source, so a multi-wavelength source can be used as the seed source to increase the swept range. However, because the circulation number is controlled by the wavelength band-pass filter, LSFS cannot realize multiple wavelengths sweeping, otherwise the swept range of different wavelength components will overlap. Recently, double circulation loops is demonstrated to be able to stitch the swept range of the seed source [23]. However, two frequency shifters increases the complexity and the cost of the system.

In this work, we use a multi-wavelength seed source to establish a synchronous lightwave synthesized frequency sweeper (SLSFS). Instead of the conventional wavelength filter, a programmable radio frequency (RF) signal that drives the frequency shifter is used to precisely control the swept range. Different frequency components of the multi-wavelength seed source sweep synchronously without overlap. The swept rate increases several times compared with single frequency swept source. Experimentally, a 120 kHz swept rate over 4.75 nm range using two coupled DFB-LDs as the seed source is achieved. The K-linearity of Pearson's correlation coefficients is 0.99999. The output of 400 kHz, 800 kHz, and 1.23 MHz swept rate over 7.86 nm range are also observed using an F-P LD as the seed source. The limitation factor of the flatness of the output is also analyzed. We show the potential to broaden the swept range to 60 nm in optimize.

2. Experimental Setup for Wavenumber Linear-Step-Swept Source Based on SLSFS

Fig. 1 shows the scheme of the wavenumber linear-step-swept source based on SLSFS. The system has two main parts: (i) a multi-wavelength laser as a seed source; (ii) a frequency synchronously swept optical loop. The seed source has multiple frequency components with fixed frequency interval, which is modulated into pulse source by an IM modulator. The number of the frequency components is depict as N in this paper. The loop includes an optical coupler (OC), a DP-MZM modulator driven by a RF signal for frequency shifting [24], a phase shifter (PS) for controlling the phase difference between the two RF ports of the DP-MZM, an isolator (ISO) for ensuring

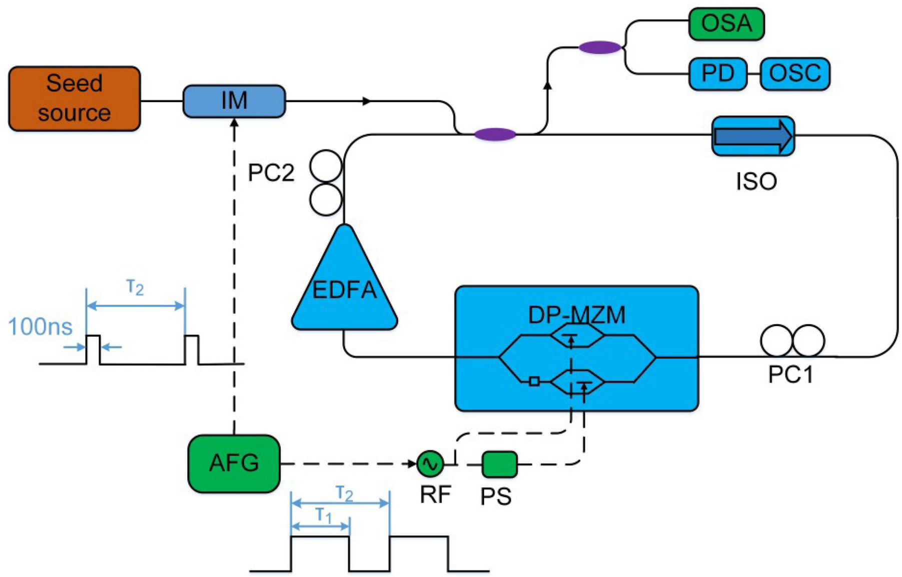

Fig. 1. The scheme of the linearly wavenumber-swept fiber laser. IM: intensity modulator; OC: optical coupler; ISO: isolator; PC: polarization controller; DPMZM: dual-parallel Mach-Zehnder modulator; EDFA: erbium-doped fiber amplifier; AFG: arbitrary function generator; RF: radio frequency; PS: phase shifter.

unidirectional light propagation, an erbium-doped fiber amplifier (EDFA) for compensating the optical loss, and two polarization controllers (PC) for controlling the polarization state of the optical signal. The DP-MZM modulator acts as a switch of the optical loop by programming the driven RF signal via an arbitrary function generator (AFG) (discussed in Sec. 3). The wavelength filter is not needed in this SLSFS. The output of the SLSFS is sent to an optical spectrum analyzer (OSA) and an oscilloscope (OSC) via a photodetector (PD). The AFG controls the IM and RF synchronously by two sequences of square pulse with the same period T_2. The width of the square pulse that controls the RF is T_1. Correspondingly, the width of another square pulse controlling the IM is set to a fixed value. In our system it is set as 100 ns.

We assume that the multi-wavelength source E_i includes N optical frequency components with equal power. E_i can be expressed as

$$E_i = \sum_{n=0}^{N-1} E_0 \exp[i2\pi(f_0 + nf_s)t], \tag{1}$$

where f_0 is the optical frequency of the first optical component, f_s is the frequency interval of the multi-wavelength seed source and E_0 is the amplitude of each optical component. E_i is shaped into pulses by applying pulse electrical signal on IM modulator and the output time is t_1. Fig. 2(a1) shows the optical spectra in k-space and Fig. 2(b1) shows the corresponding pulse waveforms in the time domain. The output of the seed source is split into two parts. One is coupled directly into the OSA and the PD, and the other one is sent into the synchronous swept optical loop for frequency shifting. In the loop, a DP-MZM modulator driven by an RF signal is used for single side band (SSB) modulation [20]. After passing the DP-MZM, the seed source is synchronously shifted in k-space with a constant value Δf. The output E_{o1} of the loop after one circulation can be expressed as

$$E_{o1} = \sum_{n=0}^{N-1} E_0 \exp[i2\pi(f_0 + nf_s + \Delta f)t]. \tag{2}$$

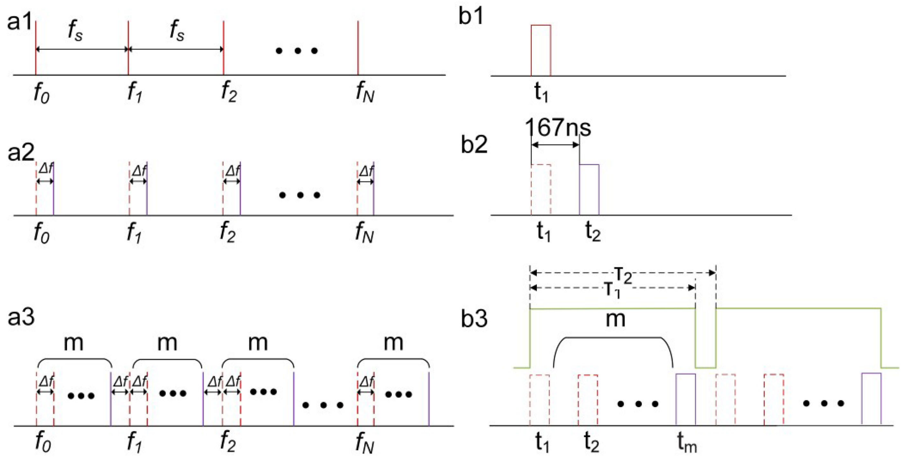

Fig. 2. The schematic diagram of the output in the frequency domain and the waveform in the time domain.

The output time is t_2, which is shown in Fig. 2(a2) and Fig. 2(b2) by the solid line. The length of the optical loop is about 33.4 m and the circulation time is about 167 ns. After *m* runs of circulation, the original seed frequency f_0 is shifted to frequency $f_1 - \Delta f$ and correspondingly, f_1 *to* $f_2 - \Delta f, \ldots f_{N-1}$ to $f_N - \Delta f$. It means that the frequency sweeping is achieved. The final output can be expressed as

$$E_{on} = \sum_{n=0}^{N-1} E_0 \exp[i2\pi(f_0 + nf_s + m\Delta f)t] \tag{3}$$

$$m = \frac{f_s}{\Delta f} - 1, \tag{4}$$

where *m* is the circulation number. The spectra and the pulse waveform of the output after *m* circulations are shown in Fig. 2(a3) and Fig. 2(b3) respectively. The width T_1 of the square pulse decides the circulation number *m* of the loop and the period T_2 of the square pulse decides the swept rate. Because both the frequency shift and the light passing time of each circulation are constant, the linearity of the swept output in the k-space can be one in theory. Compared with single frequency seed source, the swept rate increases N times within the same swept range.

3. Experimental Results and Discussion

In our experiments, two DFB-LDs (central wavelengths are 1549.801 nm and 1552.198 nm respectively) with frequency interval of 301 GHz are coupled together and used as the seed source. The output of the DFB-LDs seed source is modulated into pulses with 100 ns pulse width. As an example, the circulation number m is set to 301/8.6-1 = 34. So the swept step is 8.6 GHz. Fig. 3 shows the output spectrum of the seed source after being shifted only once by the DP-MZM modulator. The black line is the spectrum when the driven RF signal is applied. Correspondingly, when the RF signal is off, the spectrum is the red line. In Fig. 3, we can see that the two frequency components (the black line) modulated by the DP-MZM are shifted 8.6 GHz in frequency domain synchronously. The side mode suppression ratio (SMR) of each frequency component is more than 25 dB when the RF signal is on. As shown in Fig. 3, the optical power difference is larger than 27 dB between the RF signal on and off. It means that the optical signal is strongly attenuated in the optical loop when the RF signal is off. So the DPMZM modulator can act as a switch of the optical loop. The circulation number can be precisely controlled by controlling the driven RF signal. The conventional wavelength filter is not needed to control the circulation number in this SLSFS.

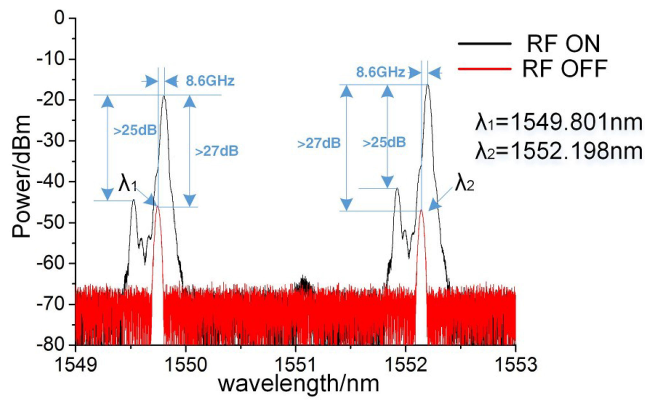

Fig. 3. The output spectrum of the seed source after being modulated once by the DP-MZM modulator (f_{RF} = 8.6 GHz).

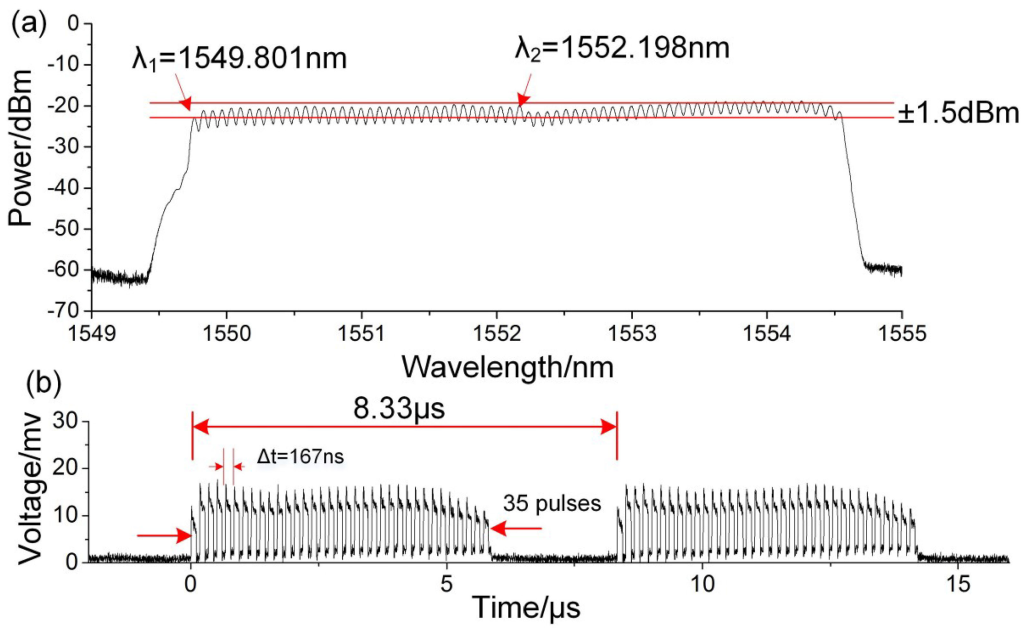

Fig. 4. The spectrum (a) and the waveform (b) of SLSFS using two coupled DFBs as a seed source (f_{RF} = 8.6 GHz).

Fig. 4 shows the swept output spectrum and the waveform of the SLSFS when the swept step is 8.6 GHz. The resolution of the OSA is 0.03 nm. When the RF is turned on, the frequencies of the two original input seed signals are swept to lower frequencies synchronously, the corresponding wavelengths are swept to longer wavelength as shown in Fig. 4(a). The flatness of the swept spectrum is ±1.5 dB within a swept range of 4.75 nm. Fig. 4(b) shows the output waveform of the optical loop in time domain. In the experiments, the width of the pulses is set as 100 ns. The length of the optical loop is about 33.4 m corresponding to the circulation time is 167 ns. The T_1 is set to 167 ns × 35 + 100 ns = 5.95 μs and the T_2 is set to 8.33 μs. The swept rate is 120 kHz (1/8.33 μs). Compared with single DFB-LD as the seed source, the swept rate increases by two times by using double DFB-LDs seed source with same swept step and swept range. The bottoms of every pulse are slightly increased as the consequence of the noise accumulation in every circulation. The linearity in the frequency domain of the swept source is analyzed with the data of the spectrum of

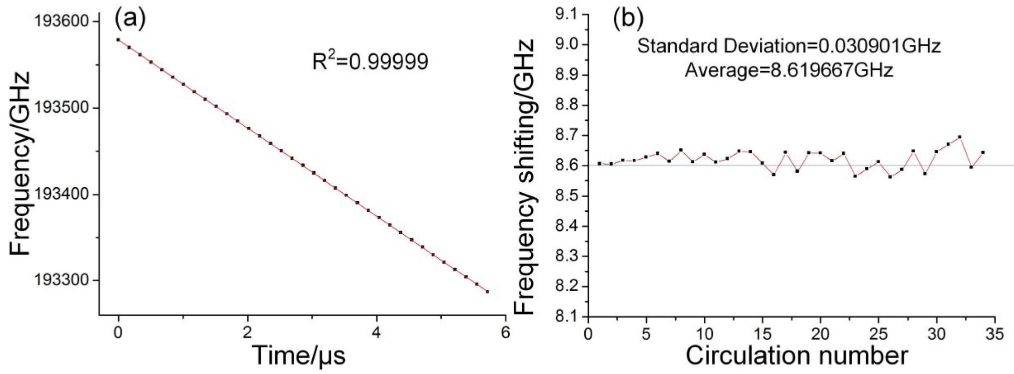

Fig. 5. Linearity (a) and frequency error (b) of the swept source using DFB-LD1 as the seed source.

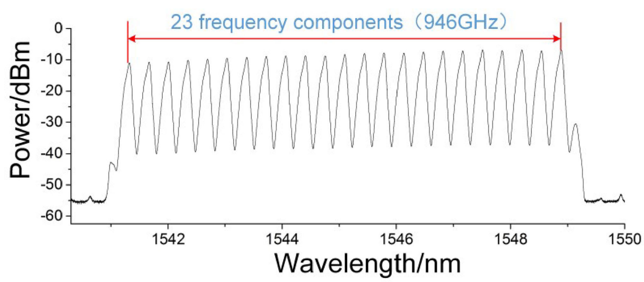

Fig. 6. The output spectrum of F-P LD.

the swept output in Fig. 4(a) and the corresponding pulse in time domain in Fig. 4(b). The linearity of swept source using DFB-LD1 ($\lambda_1 = 1549.801$ nm) as seed source is plotted in Fig. 5(a). It is nearly a perfect linearity with the Pearson's correlation coefficients 0.99999. The relative frequency error of every circulation is shown in Fig. 5(b). The average of the measured values of frequency shifting is 8.619667 GHz and the standard deviation is 0.030901 GHz. The frequency error is mainly from the phase noise of the RF signal. The measured linearity of the wavelength component, λ_2, of the swept source is also 0.99999. It implies that this SLSFS is capable of providing linearly sweeping for multi-wavelength seed source in frequency domain. The tiny nonlinearity is mainly due to the resolution of the OSA and the dispersion of the optical fiber (typically 17 ps/nm/km in a single mode fiber), which can be neglected in our system.

In another experiment, the frequency interval of the multi-wavelength seed source is changed to reduce the circulation number for higher swept rate and more wavelength components are supplied to broaden the swept range. In these experiments, the DFB-LDs are replaced by an F-P LD. A bandpass filter is used to filter out 23 frequency components of F-P LD. Fig. 6 shows the output spectrum of the F-P LD. The frequency interval between each component is 43 GHz and the output range of F-P LD is 43 GHz $\times$ 22 $=$ 946 GHz. The swept step is set to 8.6 GHz and the circulation number m is 43/8.6-1 $=$ 4. Fig. 7 shows the spectrum and the waveform of the SLSFS using the F-P LD as the seed source. The T_1 is set to 167 ns $\times$ 4 $+$ 100 ns $=$ 768 ns. By changing the period T_2 of the square pulse train, the swept rate ($1/T_2$) of the swept laser can be changed. The swept rate in Fig. 7(a-c) is 400 kHz, 800 kHz and 1.23 MHz respectively. The swept range is over 7.86 nm. Because of the limitation of the length of the optical loop, the maximum swept rate is 1.23 MHz for the F-P LD. The low frequency noise in time domain is caused by the IM modulator and DPMZM modulator.

Noticing the output flatness of the SLSFS is not as good as the F-P LD seed source, the limitation factor of the flatness of the output is analyzed. Fig. 8 shows the gain spectrum of the EDFA. The

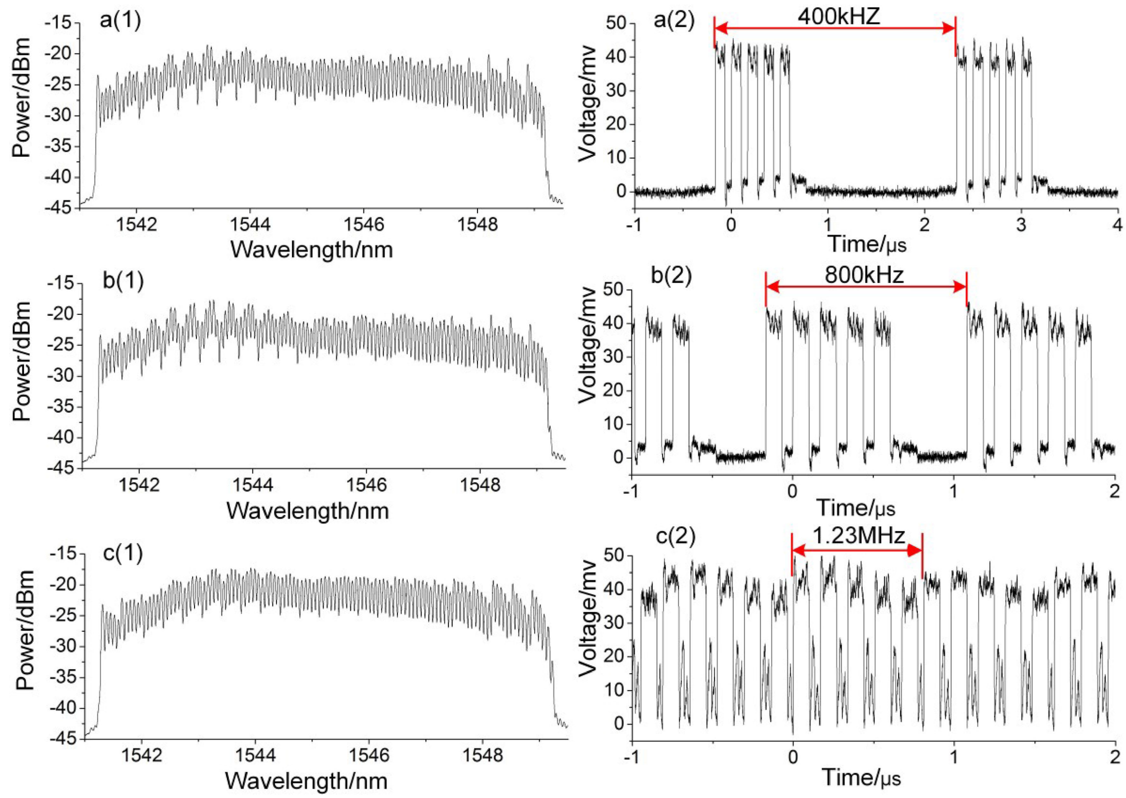

Fig. 7. The spectrum a(1), b(1), c(1) and the waveform a(2), b(2), c(2) of the SLSFS using the F-P LD as the seed source ($f_{RF} = 8.6$ GHz) at 400 kHz, 800 kHz and 1.23 MHz swept rate.

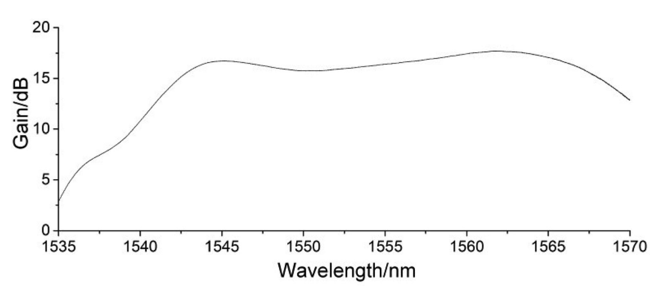

Fig. 8. The gain spectrum of the EDFA.

gain range of EDFA we used is from 1540 nm to 1550 nm. Because the gain spectrum is not flat enough, the swept flatness of the SLSFS using an F-P LD as the seed source is limited. Owing to the operating wavelength range of DP-MZM modulator that is 60 nm in our experiments, the swept output with 60 nm swept range can be achieved in theory as long as the EDFA has flat gain spectrum and enough gain bandwidth.

4. Conclusions

An ultrafast high linearity wavenumber-swept fiber laser based on a synchronously LSFS is proposed and demonstrated. The circulation number of the SLSFS is controlled by a stable programmable RF signal which is applied on a DP-MZM modulator rather than a wavelength filter. A multi-wavelength laser can be used as the seed source of the SLSFS to increase the swept rate. Using two coupled DFB-LDs as seed source, we acquired an output of 120 kHz swept rate with 0.99999 swept linearity in k-space and the swept range is over 4.75 nm. The output of 400 kHz, 800 kHz and 1.23 MHZ swept rate over 7.86 nm swept range using an F-P LD as the seed source are also achieved. The swept range can be broadened as long as the EDFA has flat gain spectrum and the gain bandwidth is wide enough. Shorter loop length can further increase the swept rate.

References

[1] Y. Nakazaki and S. Yamashita, “Fast and wide tuning range wavelength-swept fiber laser based on dispersion tuning and its application to dynamic FBG sensing,” *Opt. Exp.*, vol. 17, no. 10, pp. 8310–8318, May 2009.
[2] T. Taniguchi, N. Sakurai, H. Kimura, and K. Kumozaki, “Heterodyne detection of wavelength-swept super-dense WDM signal employing spectrum shaping,” *Electron. Lett.*, vol. 45, no. 17, pp. 902–903, Aug. 2009.
[3] J. F. De Boer, R. Leitgeb, and M. Wojtkowski, “Twenty-five years of optical coherence tomography: The paradigm shift in sensitivity and speed provided by Fourier domain OCT,” *Biomed. Opt. Exp.*, vol. 8, no. 7, pp. 3248–3280, Jun. 2017.
[4] K. Iiyama, L. wang, and K. Hayashi, “Linearizing optical frequency-sweep of a laser diode for FMCW reflectometry.” *J. Lightw. Technol.*, vol. 14, no. 2, pp. 173–178, Feb. 1996.
[5] H. Takesue and T. Horiguchi, “Very fast chromatic dispersion measurement using lightwave synthesized frequency sweeper and lock-in detection with phase diversity technique,” in *Proc. Optical Fiber Commun. Conf. Int. Conf. Quantum Inf., OSA Tech. Digest*, 2001, vol. 3, Paper WDD87.
[6] P. Lindelöw and J. J. Mohr, “Coherent lidar modulated with frequency stepped pulse trains for unambiguous high duty cycle range and velocity sensing in the atmosphere,” in *Proc. IEEE Int. Geosci. Remote Sens. Symp.*, 2007, pp. 2787–2790.
[7] S. H. Yun, “Mode locking of a wavelength-swept laser,” *Opt. Lett.*, vol. 30, no. 19, pp. 2660–2662, Oct. 2005.
[8] G. R. Lin, J. Y. Chang, Y. S. Liao, and H. H. Lu, “L-band erbium-doped fiber laser with coupling ratio controlled wavelength tunability,” *Opt. Exp.*, vol. 14, no. 21, pp. 9743–9749, Oct. 2006.
[9] S. M. R. Motaghian Nezam, “High-speed polygon-scanner-based wavelength swept laser source in the telescope-less configurations with application in optical coherence tomography,” *Opt. Lett.*, vol. 33, no. 15, pp. 1741–1743, Aug. 2008.
[10] B. Potsaid *et al.*, “Ultrahigh speed 1050 nm swept source /Fourier domain OCT retinal and anterior segment imaging at 100,000 to 400,000 axial scans per second,” *Opt. Exp.*, vol. 18, no. 19, pp. 20029–20048, Sep. 2010.
[11] C. M. Eigenwillig, B. R. Biedermann, G. Palte, and R. Huber, “K-space linear Fourier domain mode locked laser and applications for optical coherence tomography,” *Opt. Exp.*, vol. 16, no. 12, pp. 8916–8937, Jun. 2008.
[12] D. D. John *et al.*, “Wideband electrically pumped 1050-nm MEMS-tunable VCSEL for ophthalmic imaging,” *J. Lightw. Technol.*, vol. 33, no. 16, pp. 3461–3468, Aug. 2015.
[13] H. D. Lee, M. Y. Jeong, C. S. Kim, J. G. Shin, B. H. Lee, and T. J. Eom, “Linearly wavenumber-swept active mode locking short-cavity fiber laser for in-vivo OCT imaging,” *IEEE J. Sel. Topics Quantum Electron.*, vol. 20, no. 5, Sep./Oct. 2014, Art. no. 1101008.
[14] J. Ensher, P. Boschert, K. Featherston, J. Huber, M. Crawford, and M. Minneman, “Long coherence length and linear sweep without an external optical K-clock in a monolithic semiconductor laser for inexpensive optical coherence tomography,” *Proc. SPIE*, vol. 8213, 2012, Art. no. 82130T.
[15] T. Huo *et al.*, “Linear-in-wavenumber swept laser with an acousto-optic deflector for optical coherence tomography,” *Opt. Lett.*, vol. 39, no. 2, pp. 247–250, Jan. 2014.
[16] A. Vasilyev, N. Satyan, S. Xu, G. Rakuljic, and A. Yariv, “Multiple source frequency-modulated continuous-wave optical reflectometry: Theory and experiment,” *App. Opt.*, vol. 49, no. 10, pp. 1932–1937, Mar. 2010.
[17] D. Choi, R. Yoshimura, and K. Ohbayashi, “Tuning of successively scanned two monolithic vernier-tuned lasers and selective data sampling in optical comb swept source optical coherence tomography,” *Biomed. Opt. Exp.*, vol. 4, no. 12, pp. 2962–2987, Dec. 2013.
[18] T. Dilazaro and G. Nehmetallah, “Large-volume, low-cost, high-precision FMCW tomography using stitched DFBs,” *Opt. Exp.*, vol. 26, no. 3, pp. 2891–2904, Feb. 2018.
[19] M. Njegovec and D. Donlagic, “Interrogation of FBGs and FBGs arrays using standard telecom DFB diode,” *J. Lightw. Technol.*, vol. 34, no. 22, pp. 5340–5348, Nov. 2016.
[20] K. Shimizu, T. Horiguchi, and Y. Koyamada, “Frequency translation of light waves by propagation around an optical ring circuit containing a frequency shifter: I. Experiment,” *Appl. Opt.*, vol. 32, no. 33, pp. 6718–6726, Nov. 1993.
[21] K. Shimizu, T. Horiguchi, and Y. Koyamada, “Frequency translation of light waves by propagation around an optical ring circuit containing a frequency shifter: II. Theoretical analysis,” *Appl. Opt.*, vol. 33, no. 15, pp. 3209–3219, May 1994.
[22] M. Wan *et al.*, “Rapid, k-space linear wavelength scanning laser source based on recirculating frequency shifter,” *Opt. Exp.*, vol. 24, no. 24, pp. 27614–27621, Nov. 2016.
[23] J. Zhang *et al.*, “Stable optical frequency-locked multicarriers generation by double recirculating frequency shifter loops for tb/s communication,” *J. Lightw. Technol.*, vol. 30, no. 24, pp. 3938–3945, Dec. 2012.
[24] Z. Wang *et al.*, “Precise simultaneous multiwavelength tuning by electrical RF signals,” *IEEE Photon. Technol. Lett.*, vol. 25, no. 10, pp. 914–916, May 2013.